applied sciences

MDPI

Article

Study of Sea Fog Environment Polarization Transmission Characteristics

Qiang Fu [1,2,*], Kaiming Luo [1], Yu Song [1], Meng Zhang [1,2], Su Zhang [1,2], Juntong Zhan [1,2], Jing Duan [1,3] and Yingchao Li [1,2]

[1] National and Local Joint Engineering Research Center of Space Optoelectronics Technology, Changchun University of Science and Technology, Changchun 130022, China
[2] College of Opto-Electronic Engineering, Changchun University of Science and Technology, Changchun 130022, China
[3] Electronic Information Engineering, Changchun University of Science and Technology, Changchun 130022, China
* Correspondence: cust_fuqiang@163.com

Abstract: Sea fog is a particular kind of atmospheric aerosol that often poses hidden risks to ship navigation, ocean exploration, human productivity, and life. In light of the aforementioned issues, this research conducted a thorough investigation of the polarization transmission properties in a sea fog environment. We studied the physical characteristics of sea fog and established a polarized radiative transfer model based on RT3/PolRadtran (polarized radiative transfer) in a sea fog environment based on the theory of Mie scattering. The effects of wavelength, polarization state, sea fog concentration, and salt content on the polarization degree were simulated by using the polarization transport model. An indoor sea fog simulation device was designed and built. The simulation test results were compared with the experimental test results from many aspects, and the existing errors were analyzed so that they could be mutually verified for the overall trend. According to the modeling results, distinct polarization states of light exhibit evident depolarization as the sea fog concentration rises. Overall, circularly polarized light has superior polarization-maintaining properties compared to linearly polarized light under the same contrast settings. The penetrating impact of incoming light in the visible range improves with increasing wavelength, and the amount of salt in sea fog has some bearing on the degree of polarization.

Keywords: Mie scattering; optical thickness; polarization; sea fog; transmission

Citation: Fu, Q.; Luo, K.; Song, Y.; Zhang, M.; Zhang, S.; Zhan, J.; Duan, J.; Li, Y. Study of Sea Fog Environment Polarization Transmission Characteristics. *Appl. Sci.* **2022**, *12*, 8892. https://doi.org/10.3390/app12178892

Academic Editor: Andrey Miroshnichenko

Received: 9 August 2022
Accepted: 30 August 2022
Published: 5 September 2022

1. Introduction

Sea fog is a kind of condensation phenomenon that develops when a lot of water vapor condenses in the lower atmosphere as a result of saltwater evaporation. Polarized light interacts with complicated energies during transmission, such as collision and scattering with nearby sea fog particles, changing the amount of information conveyed by light transmission in the sea fog. Studying the polarized light transmission properties of sea fog particles is thus crucial for maritime exploration.

Light will scatter, refract, or absorb in the medium as it moves through it. Polarized light, which is often more effective in carrying information about the target, is created when natural light scatters across the medium. As a result, several academics from both home and abroad have consistently conducted studies on polarization features in complex contexts [1–4]. By examining the impact of altering the size and distribution of fog particles under scattering environment conditions (such as fog), Wright et al. [5] performed a series of Monte Carlo simulations of polarized light with monodisperse particle size and different particle size distributions as scattering environment models. The persistence of the circumference and radius of linearly polarized light was also simulated. LaCasse C F et al. [6] proposed that the particle size, waveform length, refractive index, and detection range may

all be altered when using polarization-tracking Monte Carlo simulation. Circular polarization propagates more effectively in radiation and advection fog, according to research, than linear polarization. Zeng, X. et al. [7] proposed four MODTRAN fog models (moderate and severe radiation and moderate and severe advection fog), and four real-world-observed fog particle distributions were used to simulate polarized light propagation in fog. By resolving the vector radiative transfer equation, Yang, B. et al. [8] quantitatively evaluated the polarization radiation properties of the sea fog layer. By combining the scattering data of sunlight in the air and sea environment, Sun, X.M. et al. [9] were able to obtain the polarization reflection function of the entire atmospheric top and analyze the sensitivity of the reflection function to the wavelength, observation geometry, sea surface and ocean characteristics, aerosol and cloud microphysics, and optical characteristics. Sea surface flare is a significant source of interference in the identification of ocean objects, according to Chen, W. et al. [10], who examined the polarization properties of targets against a sea surface flare background.

The majority of current research on sea fog focuses on the composition, distribution, and other key aspects of sea fog, with less attention being paid to its optical qualities and more attention being paid to the radiation and extinction properties of marine aerosols [11]. Studies on polarization transmission properties in sea fog environments are few. A polarization transmission model based on the RT3 sea fog environment was built in order to broaden the application range of polarization detection and further investigate the transmission properties of polarized light in complicated maritime environments. The results provide theoretical and technical support for high-precision imaging detection of marine targets by simulating the polarization characteristics of various wavelengths, polarization states, sea fog concentrations, and salt contents. One should also confirm the evolution law of vertical polarization transmission characteristics in multi-layer marine media environments.

2. The Physical Attributes of a Complicated Environment such as Marine Fog

2.1. Marine Fog's Physical Qualities

The production of marine fog depends on the temperature of the sea air, the amount of water vapor present, and the presence of condensation nuclei. Sea fog is significantly distinct from most clouds in that it achieves air supersaturation by adiabatic cooling, which lowers air pressure. Sea fog does not arise primarily as a result of air pressure in the lower atmosphere close to the ground. In further detail, if f represents the relative humidity of the air, it is defined as the proportion of the saturated water vapor pressure e_a at the actual temperature T to the real water vapor pressure e, and its related representation is as follows [12]:

$$f = \frac{e}{e_a} \tag{1}$$

The derivative is derived by applying logarithms to both sides of the preceding formula:

$$\frac{df}{f} = \frac{de}{e} - \frac{de_a}{e_a} \tag{2}$$

Let L represent the latent heat of evaporation, A represent the heating equivalent, and R_W represent the specific gas constant of water vapor, which are put into the Clausius–Clapeyron equation.

$$\frac{de_a}{e_a} = \frac{L}{AR_W}\frac{dT}{T^2} \tag{3}$$

Combining (2) and (3):

$$\frac{df}{f} = \frac{de}{e} - \frac{L}{AR_W}\frac{dT}{T^2} \tag{4}$$

If T = 273 K and $\frac{L}{AR_WT} \approx 19.5$, then Formula (4) is:

$$\frac{df}{f} = \frac{de}{e} - 19.5\frac{dT}{T^2} \tag{5}$$

Equation (5) demonstrates that the relative humidity in a marine environment can be raised to saturation by raising the water vapor pressure and decreasing the temperature. In the process of marine fog generation, two distinct processes often act in tandem. Humidification in the marine environment occurs primarily through seawater evaporation and atmospheric precipitation, whereas cooling is primarily of two types: the sea surface temperature is lower than the atmospheric temperature, or there is a temperature difference between the sea surface and the atmosphere.

2.2. Fundamental Method for Polarization Transmission in Marine Environments

In a sea fog environment, polarized light collides with particles of sea fog during transmission, resulting in refraction, absorption, and scattering, which significantly reduces the polarization intensity of polarized light. If the diffuse reflection induced by multiple scattering is disregarded, the intensity change law of light radiation can be written directly as [13]:

$$\frac{dI_\lambda}{k_\lambda \rho d_s} = -1 \tag{6}$$

According to Equation (6), the incident wavelength is λ. The intensity of the radiation (I_λ), the coefficient of extinction cross-section (k_λ), the thickness of the medium during transmission (s), and the density between particles (ρ) are required. When $s = 0$, $I_\lambda(0)$ represents the initial light wave radiation intensity of incoming light. When $s_1 \neq 0$, it shows the intensity of light wave radiation after transmission through a medium of thickness s_1.

$$I_\lambda(s_1) = I_\lambda(0)exp(-\int_0^{s_1} k_\lambda \rho d_s) \tag{7}$$

If the transmission medium is spread evenly, the extinction section coefficient k_λ is independent of distance s_l, and the transmission route length can be calculated as follows:

$$\mu = \int_0^{s_1} \rho d_s \tag{8}$$

Introducing Formula (8) into Formula (7), the relationship between incoming radiation intensity and emitted radiation intensity is as follows:

$$I_\lambda(s_1) = I_\lambda(0)exp(-k_\lambda \mu) \tag{9}$$

In a homogeneous medium environment, the intensity attenuation of the radiation transmission of light waves follows an exponential distribution, and the exponential independent variable is the product of the extinction coefficient and the path, as determined by the preceding Formula (9). This is Lambert's law.

Currently, most radiative transfer models in the United States and overseas alter their parameters in the vertical direction, and there is no examination of horizontal atmospheric parameters. According to their physical definitions, the horizontal optical characteristics and radiation intensity of the atmosphere are the same in all models. If Z is used to denote the longitudinal space distance, the atmospheric radiative transfer equation can be expressed more generally as follows:

$$\cos(\theta)\frac{dI(z;\theta,\varphi)}{k\rho dz} = -I(z;\theta,\varphi) + J(z;\theta,\varphi) \tag{10}$$

where θ represents the zenith angle, φ represents the azimuth, and J represents the source function. Similarly, if we want to address the multiple scattering of light in an environment of sea fog, we must incorporate the atmospheric optical thickness of light transmission in the vertical direction:

$$\tau = \int_z^\infty k\rho dz \tag{11}$$

The fundamental equation of radiation transmission based on the multiple scattering issue under the premise that the earth's atmospheric plane is parallel is derived by the calculation:

$$\mu \frac{dI(z;\theta,\varphi)}{d\tau} = -I(z;\theta,\varphi) + J(z;\theta,\varphi) \tag{12}$$

In Equation (12), μ represents the cosine of zenith angle θ.

3. Polarization Transmission of Marine Fog Simulation Based on RT3

3.1. Radiative Transfer Vector Equation

The radiative transfer equation (RTE) is a fundamental equation that defines how electromagnetic waves travel through a medium and are redistributed through absorption and scattering. It is separated into vector and scalar radiative transfer equations. Polarization is the phenomenon in which the vibration vector of a shear wave is skewed in certain directions. We are aware that a scalar has no direction, but polarization information is a vector with direction. Using the scalar radiation transmission formula to calculate the polarization transmission equation will result in the loss of polarization information. Therefore, the vector radiative transfer equation with the Stokes vector can be employed to solve the polarization transfer equation in order to increase calculation precision.

The light scattering and polarization transmission process of polarized light in the sea fog layer can be represented by the following vector radiative transfer equation [13]:

$$\mu \frac{dI(\tau,\mu,\phi)}{d\tau} = -I(\tau,\mu,\phi) + \frac{\omega}{4\pi}\int_0^{2\pi}\int_{-1}^{1} m\left(\tau,\mu,\phi;\mu',\phi'\right) I\left(\tau,\mu',\phi'\right) d\mu' d\phi' + \frac{\omega}{4\pi} F_0 \exp\left(\frac{-\tau}{\mu_0}\right) m\left(\tau,\mu,\phi';-\mu_0,\mu\phi_0\right)[1,0,0,\ 0]^T + (I-\omega)B(T)[1,0,0,\ 0]^T \tag{13}$$

The definitions and purposes of each parameter are detailed in Table 1 below.

Table 1. The parameters and definitions of the vector radiative transfer equation.

Parameter	Meaning
μ	To indicate direction, the cosine of the zenith angle is often stated as positive or negative. Downward is positive, while upward is negative.
τ	Optical density of medium
φ	Medium's optical thickness
ω	Radiation flux incident at the top of the atmosphere from the sun
F_0	Solitary scattering albedo
φ_0, μ_0	Sum of the azimuth and cosine of the solar zenith angle
B	Planck operation
m	Mueller matrix

In Formula (13), $\frac{\omega}{4\pi}\int_0^{2\pi}\int_{-1}^{1} m(\tau,\mu,\phi;\mu',\phi')I(\tau,\mu',\phi')d\mu' d\phi'$ represents the intensity of the multiple scattering of radiation, $\frac{\omega}{4\pi}F_0 \exp\left(\frac{-\tau}{\mu_0}\right) m(\tau,\mu,\phi';-\mu_0,\mu\phi_0)[1,0,0,\ 0]^T$ represents the intensity of light wave radiation at the upper border of the transmission layer, and $(I-\omega)B(T)[1,0,0,\ 0]^T$ represents air thermal radiation, which is often disregarded due to its minimal contribution. These three expressions pertain to atmospheric scattering. This study calculates the first and second terms in great detail.

The Mueller matrix M is transformed into the following formula:

$$M = L(\pi - i_2) * P * L(-i_2) \tag{14}$$

When the scattering particle is spherical, the scattering phase matrix P has just four variables, and its value can be determined using joint Legendre. P can be expressed as:

$$P = \begin{bmatrix} a_1 & b_1 & 0 & 0 \\ b_1 & a_2 & 0 & 0 \\ 0 & 0 & a_3 & b_2 \\ 0 & 0 & -b_2 & a_4 \end{bmatrix} \tag{15}$$

In Equation (16), L equals:

$$L = \begin{bmatrix} 1 & 0 & 0 & 0 \\ 0 & \cos 2i & \sin 2i & 0 \\ 0 & -\sin 2i & \cos 2i & 0 \\ 0 & 0 & 0 & 1 \end{bmatrix} \tag{16}$$

In general, we employ the Fourier transform to decompose the Stokes vector I and Mueller matrix to improve the dependability of radiation transmission's intermediate variables. This is the particular expansion form:

$$I = \sum_{m=0}^{m} \begin{bmatrix} I_m \cos m(\phi - \phi_0) \\ Q_m \cos m(\phi - \phi_0) \\ U_m \sin(\phi - \phi_0) \\ \sin(\phi - \phi_0) \end{bmatrix} \tag{17}$$

$$M = \frac{1}{2}C_0 + \sum_{m=1}^{m} [C_m \cos m(\phi - \phi\prime) + S_m \sin m(\phi - \phi\prime)] \tag{18}$$

In Formula (18), C_m and S_m represent m-order Fourier mode coefficients. Expression (13) can be represented as:

$$\mu \frac{d\overline{I_m}(\tau, \mu)}{d\tau} = -\overline{I_m}(\tau, \mu) + \overline{J_m}(\tau, \mu) \tag{19}$$

where J_m is defined as:

$$\overline{J_m}(\tau, \mu) = \frac{\omega}{4} \int_{-1}^{1} m_m(\tau, \mu, \mu\prime) I_m(\tau, \mu) d\mu\prime + \frac{(1-\delta_{0m})}{2} \frac{\omega}{4\pi} \exp(\frac{-\tau}{\mu_0}) \overline{m_m}(\tau, \mu; -\mu_0) \vec{F_0} \tag{20}$$

In lieu of a direct numerical solution, this kind of vector problem is often discretized before being solved. Due to the nonlinear nature of the vector radiation equation, it is easy to lose data during the computation process, resulting in significant mistakes. The categorization of vector radiation equations is determined by the variation in their solution techniques. The predominant modalities of atmospheric radiation include Monte Carlo [14], RT3 mode, SBDART mode, and streamer mode. The RT3 mode was chosen for this work.

3.2. RT3-Based Polarization Transmission Simulation of Marine Fog

By analyzing the environment of sea fog, a polarization transmission model of sea fog was developed, which is suitable for the quantitative study of four factors: the salt content, optical thickness, wavelength, and polarization state of sea fog. According to the specifications of the RT3 model, the input sea fog layer file and the horizontal coordinate system must be calculated in advance. The flowchart in Figure 1 depicts polarization modeling based on the sea fog environment in China [15].

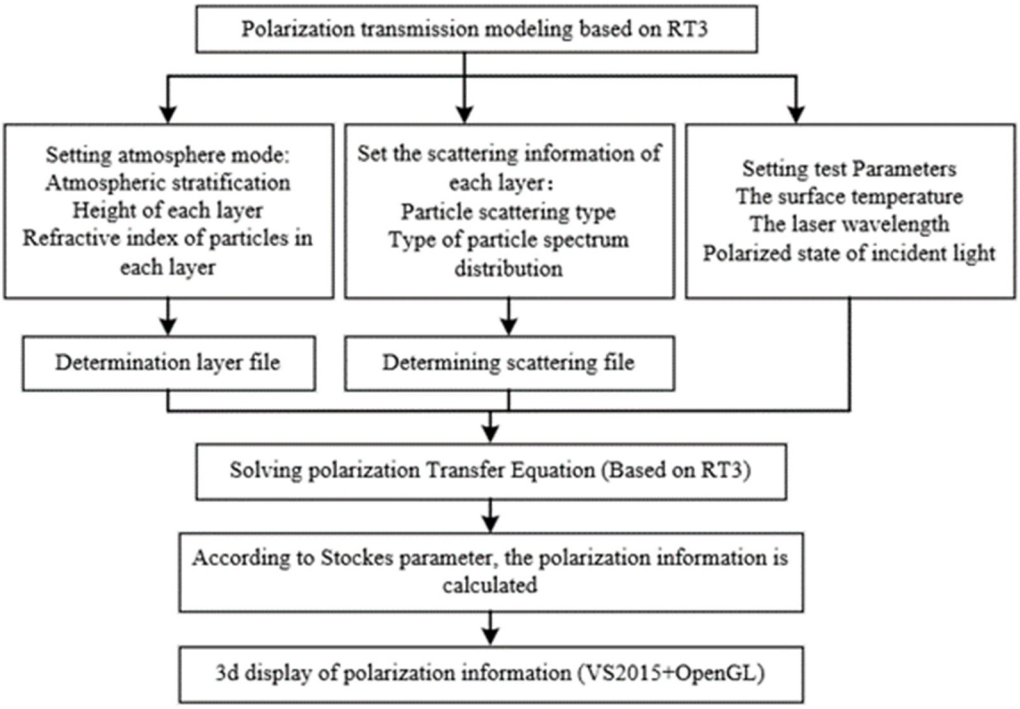

Figure 1. Flowchart of the modeling of sea fog polarization based on RT3.

In accordance with the flowchart, the layer file including the layer height and refractive index and the scattering file containing the particle scattering type and particle size spectrum distribution must be calculated prior to the simulation. The simulation and test settings are set after these calculations. According to parameter changes, the polarization transfer equation calculates distinct layer files and scattering files. This study compares and analyzes the simulation output files, sketched curves, and experimental data. OpenGL can be used to create a three-dimensional display so that the findings are simple to interpret.

3.3. Model Validation of Polarization Transmission

This research also demonstrates the accuracy of setting RT3 under cloudy and wet conditions. The particles are dispersed evenly. For calculation purposes, the simplified two-layer atmosphere is viewed as a single layer. The scattering coefficient of air molecules varies with the wavelength of the incoming light, and the model parameters are allocated accordingly. Settings were input according to Table 2, and then simulation results were processed and evaluated.

Table 2. Validation parameter values for simulation model.

Parametric	Value
Wavelength of incident light	450 nm
Optical thickness	1
Surface albedo	0.99
The scattering coefficient	$k = 1.44 * 10^{-6} * \lambda$
The surface temperature	300 K
Angle of incidence	$\theta_0 = \arccos(0.2)$

The test findings are shown in this publication as a curve for ease of viewing. The test results are shown in Figure 2. The test particles follow a gamma distribution, with an effective radius of 0.20 m on average.

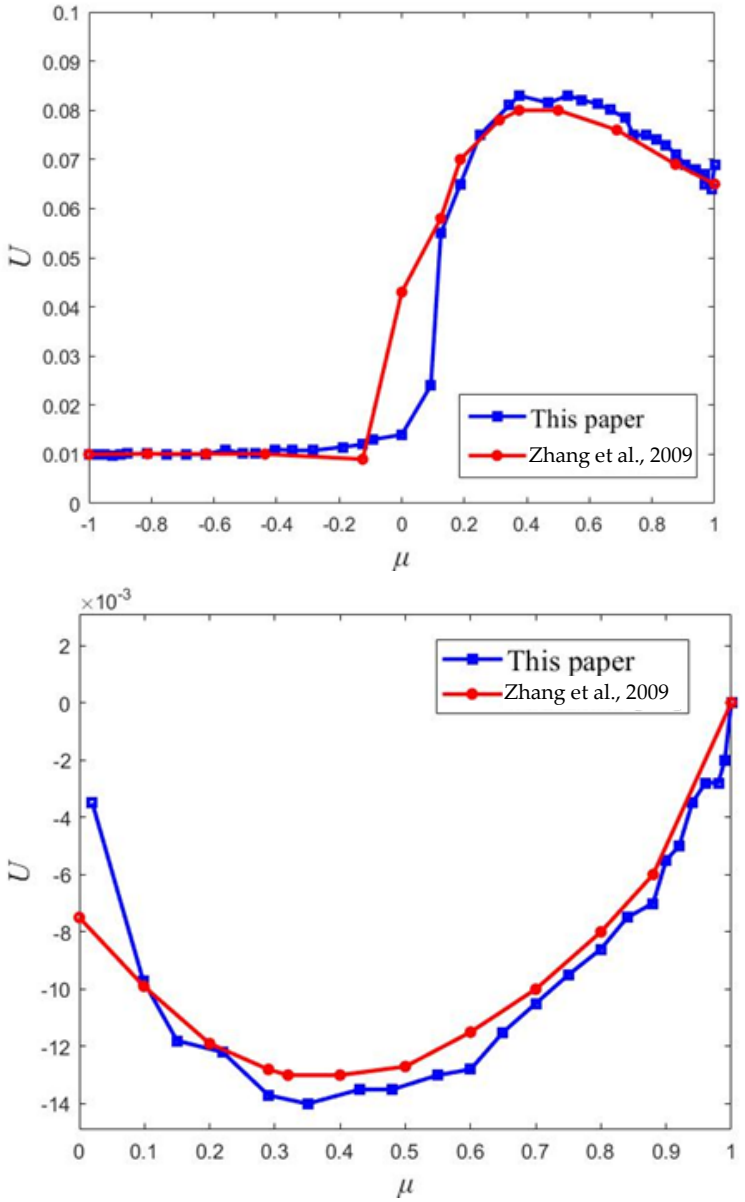

Figure 2. *I* and *V* component values in the 90° direction of the bottom circumferential angle of the atmosphere [16].

Figure 2 demonstrates that the findings for the *I* and *V* components predicted using the sea fog polarization transmission model presented in this work are mostly similar to published results. When the optical thickness is small, there is some discrepancy between the findings shown in this article and those in the references, but as the optical thickness increases, the general trend of the results presented in this research is consistent with those in the literature.

From the fitting of the two curves above, it is evident that the simulation results in this paper are essentially consistent with the results in the literature [16], indicating that the sea fog polarization transmission model based on RT3 described in this paper is accurate for calculating the radiative transmission of scattering media.

4. Experimental Device

The experimental device for studying polarization transmission characteristics in an indoor sea fog environment consists primarily of three components [17]: a transmitter that can control the wavelength and polarization of incident light; a sea fog environment simu-

lator that can adjust the particle size and salt concentration in sea fog; and a polarization state and optical power-receiving device, or the receiving end.

The transmitting end consists primarily of three instruments: 450 nm, 532 nm, and 671 nm lasers, attenuators that adjust the intensity of the incident laser, visible-light-band polarizers that polarize the incident laser, and wave plates that are circularly polarized light with an additional linearly polarized light phase. The main component of the apparatus for simulating a sea fog environment is the sea fog box. The top box contains the atmospheric medium, whereas the bottom box contains marine fog. The laser is emitted from the top of the box, and the primary optical channel is dispersed longitudinally. Together with the usual air medium and sea fog particles, it disperses and settles to the bottom of the box. In the experiment, the constructed simulation apparatus was used to recreate the environment of marine fog. The experiment-required sea fog environment with varying concentrations is created by adjusting the fog filling time, and the sea fog concentration is related to the fog filling time. The receiving end consists primarily of two instruments: a polarization state measurement device for measuring the polarization state of the emitted light and an optical power measurement instrument, i.e., an optical power meter. Figures 3 and 4 depict the block design and physical diagram of the polarization transmission experiment, respectively.

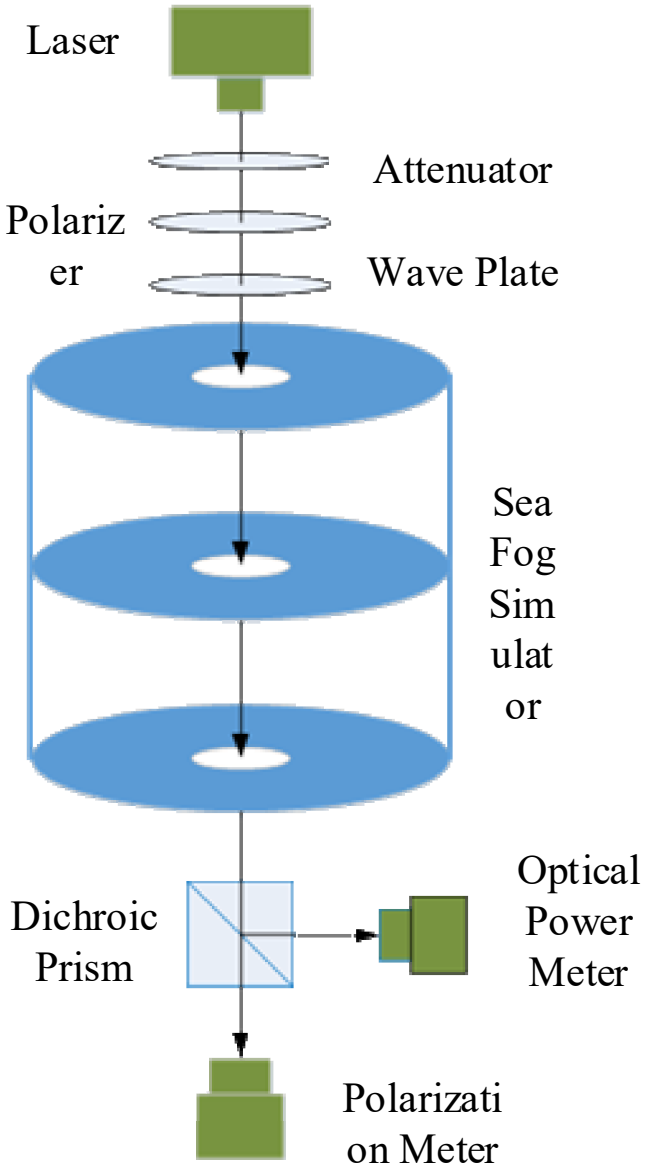

Figure 3. Schematic representation of the polarization transmission experiment.

Figure 4. A physical representation of the polarization transmission characteristic test setup.

5. Experimental Results and Analysis

(1) Salt content effect on polarization degree

The existence of sufficient condensation nodules is crucial to the production of marine fog. There are no contaminants or dust particles that can serve as condensation nodules. Even if it approaches saturation, condensation will not occur. Even when air is oversaturated eightfold (i.e., 800 percent relative humidity), only a small quantity of water condenses. In maritime environments, the condensation core is mostly composed of sea salt particles. In order to examine the effect of salt content on polarized light transmission in sea fog, three types of salt fog with varying salt contents were chosen and compared to pure water fog (0 g/L salt content). The relative NaCl concentrations were 10 g/L, 20 g/L, and 30 g/L [18]. The polarization change curve at the same wavelength was drawn but with varying salt concentrations and optical thicknesses. Figures 5–7 illustrate the relationship between the salt concentration in fog and the degree of polarization in relation to the change in optical thickness when the polarization state of three incoming wavelengths (450 nm, 532 nm, and 671 nm) is left-handed.

Figures 5–7 demonstrate that the degree of polarization decreases as the optical thickness of the four concentrations of sea fog increases. The results indicate that in the visible light range, the salt content in the fog has an effect on the polarization transmission characteristics as the optical thickness increases, and when the optical thickness remains constant, the polarization degree of the three salt fog concentrations is greater than that of the water fog. The cause is examined. The condensation nodules (salt particles) in sea fog affect the production of sea fog droplets when the fog filling time is constant. The salt in the sea fog may increase the development of fog droplets, alter their radius and quantity, and alter absorption and scattering as a result. Upon comparing the simulation results curve to the experimental results curve, it is discovered that there is an inaccuracy. The reason for this is that the sea fog environment in the experiment was not completely static

throughout the steady period and was only somewhat uniform during this time. Because the general decreasing trend is consistent with the modeling results, the experimental error is acceptable within the fault tolerance range.

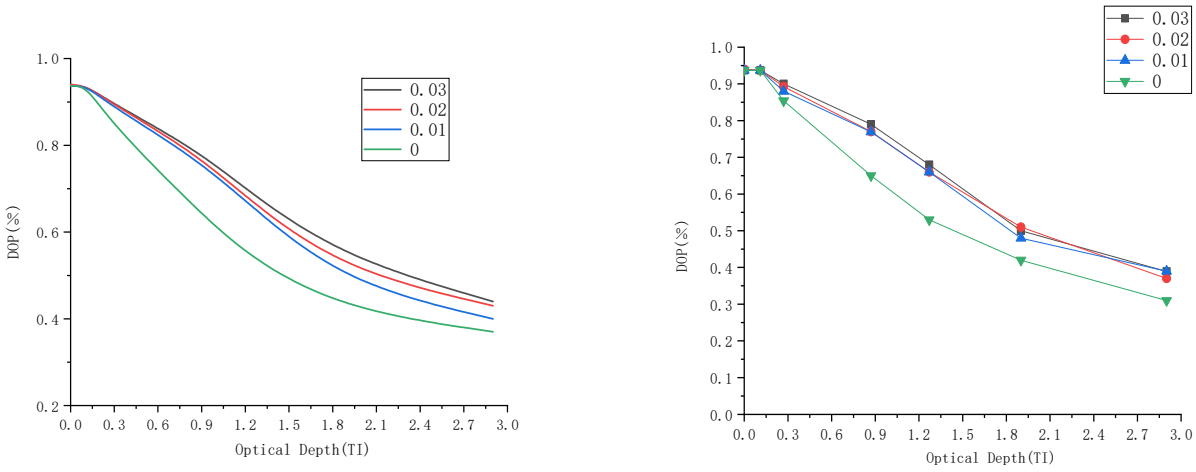

Figure 5. Simulation and experimental comparison of the relationship between salt content at 450 nm and DOP: (**a**) simulation results and (**b**) experimental results.

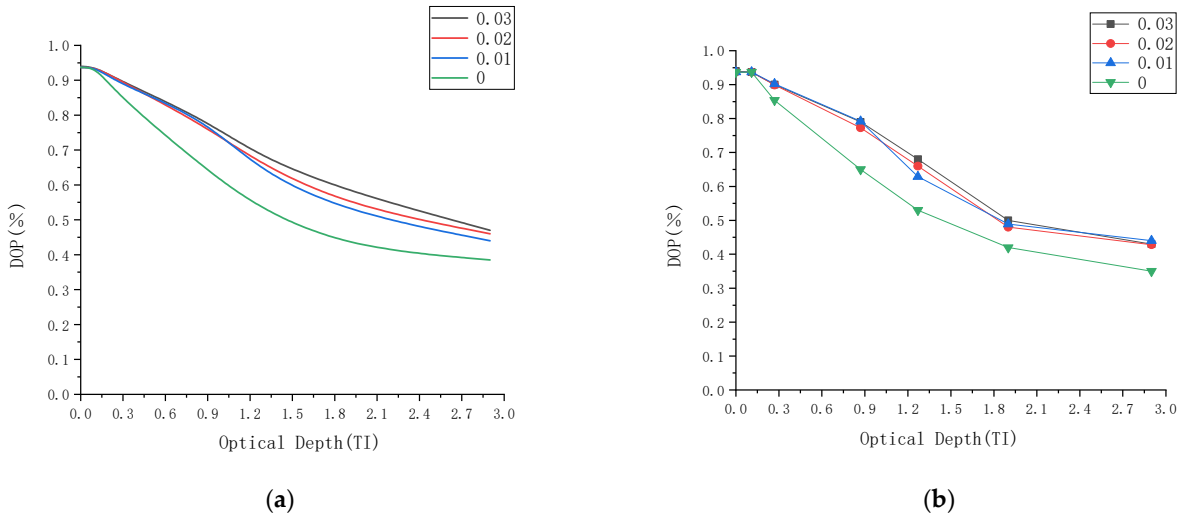

Figure 6. Simulation and experimental comparison of the relationship between salt content at 532 nm and DOP: (**a**) simulation results and (**b**) experimental results.

(2) The impact of the polarization condition of incident light on the polarization degree

In this part, the 30 g/L salt content data group is discussed, and modeling and experimental findings are assessed based on the starting polarization state and incoming light wavelength. Figures 8–10 depict the comparison of simulation and experimental results of the change in polarization degree with the increase in optical thickness during the transmission of polarized light at three incident wavelengths (450 nm, 532 nm, and 671 nm) in sea fog particles, with Figure (a) representing the simulation results and Figure (b) representing the experimental results.

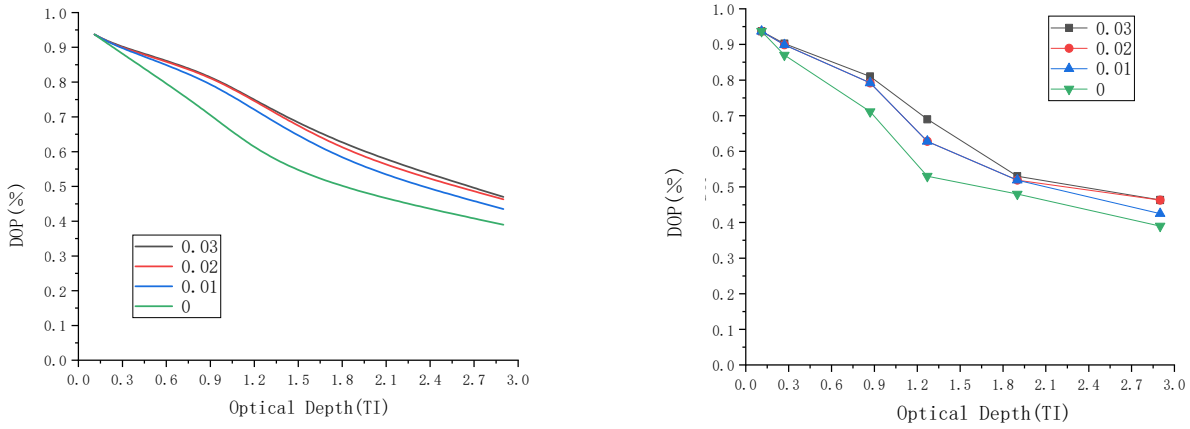

Figure 7. Simulation and experimental comparison of the relationship between salt content at 671 nm and DOP: (**a**) simulation results and (**b**) experimental results.

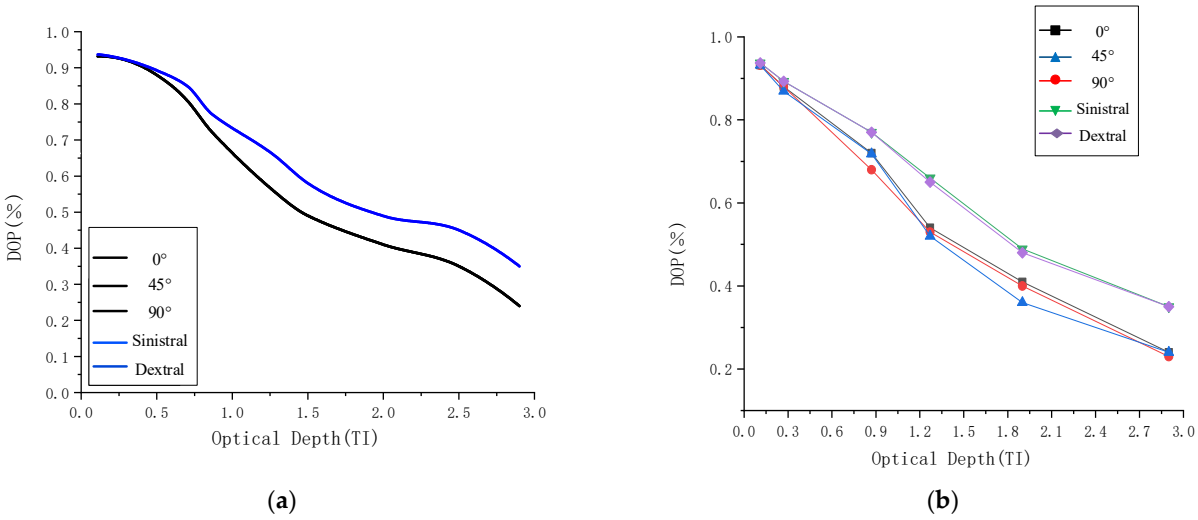

Figure 8. λ = Simulation and experimental comparison of DOP change of 450 nm polarized light: (**a**) simulation results and (**b**) experimental results.

Figure 8 demonstrates that when optical thickness increases, the degree of polarization of incoming light in five distinct polarization states decreases. In the simulation results of the three bands, the polarization state curves of 0°, 45°, and 90° incident light are completely coincident, as are the left-hand and right-hand curves. However, in the experimental results, the existence of the three curves is not precisely the same, especially as the optical thickness increases. Circularly polarized light offers superior polarization retention. The experimental outcomes are essentially in line with the simulated outcomes.

The effect of the incoming light wavelength on the polarization degree.

In this section, the 30 g/L salt content data group is discussed. In order to understand the effect of wavelength on the degree of polarization during polarized light transmission, modeling and experimental findings are studied based on the starting state of polarization and three incoming light wavelengths. The modeling and experimental curves of the degree of polarization of polarized light with varying wavelengths, optical thicknesses, and polarizing angles are shown in Figures 11 and 12. Figure 11 compares simulation and experimental results for 0° linearly polarized light in three bands, while Figure 12 compares simulation and experimental results for left-handed circularly polarized light in three bands.

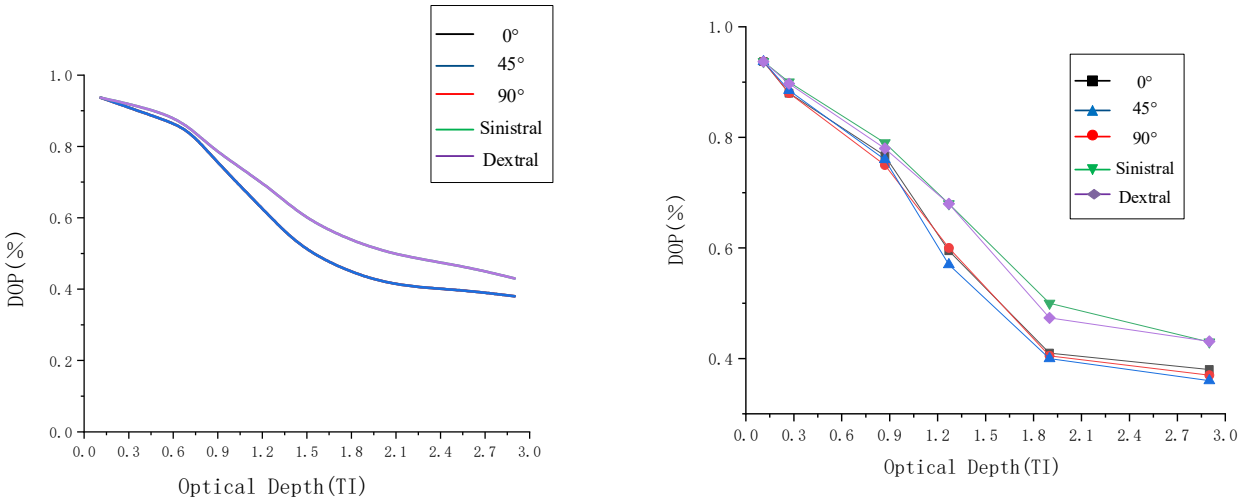

Figure 9. λ = Simulation and experimental comparison of DOP change of 532 nm polarized light: (**a**) simulation results and (**b**) experimental results.

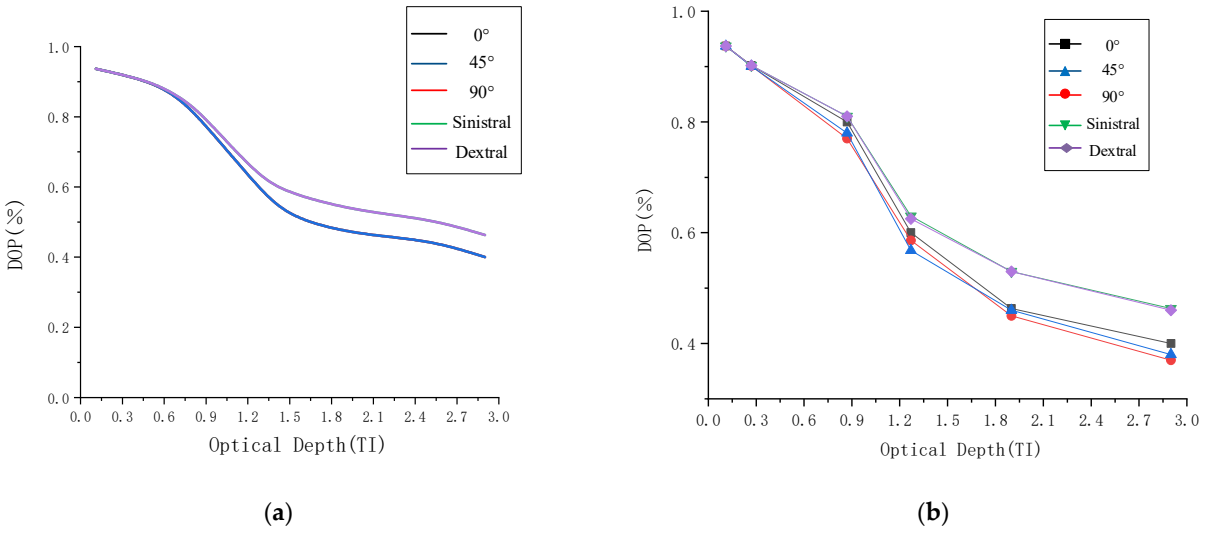

Figure 10. λ = Simulation and experimental comparison of DOP change of 671 nm polarized light: (**a**) simulation results and (**b**) experimental results.

Figure 11 depicts the variation in the degree of polarization of polarized light of different wavelengths with optical thickness when the incident light has a linear polarization angle of 0 degrees, and Figure 12 depicts the variation in the degree of polarization of polarized light of different wavelengths with optical thickness when the incident light has a left-handed circular polarization angle of 0 degrees. Figure a depicts the simulation outcome, whereas Figure b depicts the experimental outcome. From a comparison of the results curves in Figures 11 and 12, it is clear that the degree of polarization of the polarized light of the three wavelengths decreases as the optical thickness increases, and the change trend is almost the same. When the optical thickness is modest, the degree of circular polarization or linear polarization at various wavelengths does not vary noticeably. However, when the optical thickness grows, the following relationship holds for the degree of polarization of the three bands:

$$\mathrm{Dop}_{450} < \mathrm{Dop}_{532} < \mathrm{Dop}_{671}$$

In other words, when the optical thickness of the sea fog increases in the visible light spectrum, the longer the wavelength, the greater the polarization preservation, and the degree of polarization of circularly polarized light is much more than that of linearly polarized light.

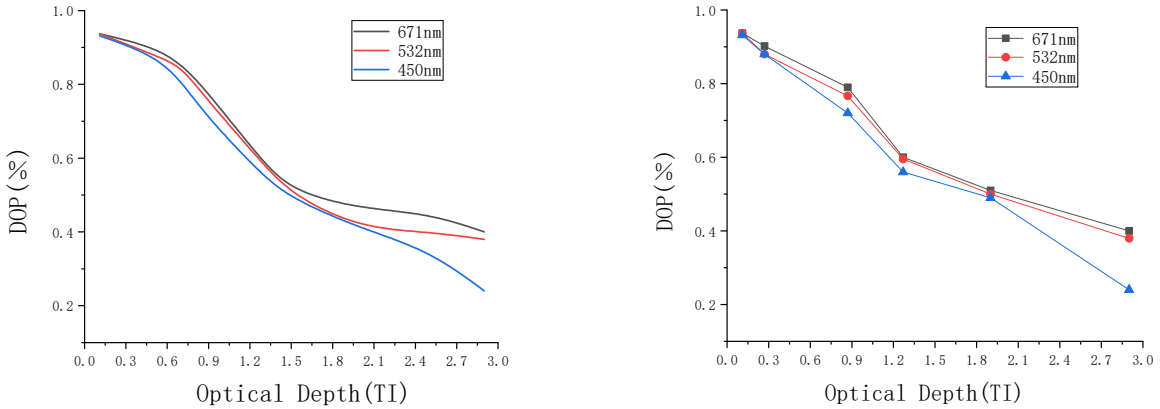

Figure 11. Simulation and experimental comparison of DOP changes in three bands when the incident light is 0-degree linearly polarized light: (**a**) simulation results and (**b**) experimental results.

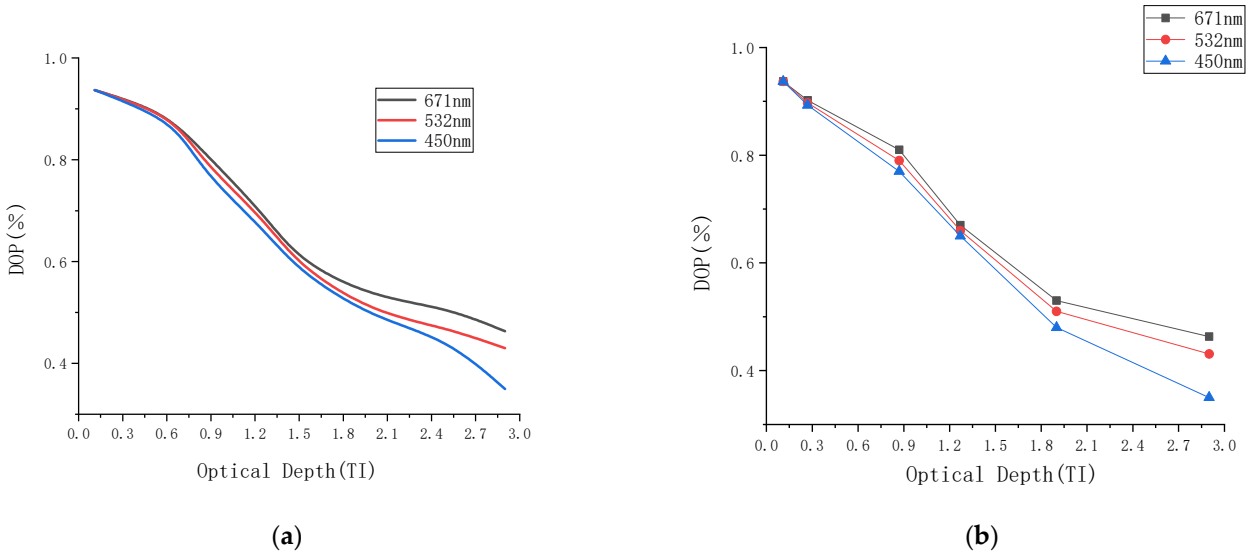

Figure 12. Simulation and experimental comparison of DOP changes in three bands when the incident light is left-handed circularly polarized light: (**a**) simulation results and (**b**) experimental results.

6. Conclusions

In this paper, firstly, the physical characteristics of sea fog are studied. Based on the basic principle of polarization transmission characteristics in a sea fog environment, a simulation model of polarization transmission characteristics in a sea fog environment was established, and the polarization transmission characteristics in different environments were tested. The established model is effective and accurate in different scattering states of sea fog. The results indicate that salt fog has a significant impact on the formation and distribution of sea fog in three salt fog and water fog environments with varying salt concentrations and that, for a given optical thickness, the polarization of polarized light transmission is greater in salt fog than in water fog. In the setting of sea fog, circularly polarized light induces rotational symmetry, which improves its polarization-maintaining properties, and the greater the penetrating impact, the longer the wavelength. With increasing optical thickness, the polarization-maintaining quality of 671 nm polarized light

improves, making it more appropriate for use in environments with sea fog. This study establishes a theoretical foundation for the transmission properties of polarized light in a multi-layer sea fog environment. However, the factors that affect the sea fog environment are not comprehensive in this paper, and temperature, non-uniform shape, and other factors can be added later.

Author Contributions: Data curation, K.L. and M.Z.; formal analysis, Y.S. and J.D.; funding acquisition, Q.F. and J.Z.; methodology, Q.F. and S.Z.; project administration, Q.F. and Y.L.; resources, Q.F. and K.L.; supervision, Q.F.; writing—original draft, K.L.; writing—review and editing, K.L. All authors have read and agreed to the published version of the manuscript.

Funding: This research was funded by Changchun University of Science and Technology, China. Huilin Jiang, National Natural Science Foundation of China, grant number 61890963.

Institutional Review Board Statement: Not applicable.

Informed Consent Statement: Not applicable.

Data Availability Statement: The study did not report any data.

Conflicts of Interest: The authors declare no conflict of interest.

References

1. Yu, T. Study on the Transmission Characteristics of Polarized Light in Ellipsoidal Particle Smoke. Master's Thesis, Changchun University of Science and Technology, Changchun, China, 2019.
2. Ahlquist, N.C.; Charlson, R.J. Measurement of the wavelength dependence of atmospheric extinction due to scatter. *Atmos. Environ.* **1969**, *3*, 551–564. [CrossRef]
3. Akritas, M.G.; Bershady, M.A. Linear Regression for Astronomical Data with Measurement Errors and Intrinsic Scatter. *Astrophys. J.* **1996**, *470*, 706. [CrossRef]
4. Rycroft, M.J. *Remote Sensing of the Lower Atmosphere*; Stephens, G.L., Ed.; Oxford University Press: Oxford, UK, 1994; 523p, ISBN 0-19-508188-9.
5. Wright, J.B.; van der Laan, J.D.; Sanchez, A.; Kemme, S.A.; Scrymgeour, D.A. Optical characterization of the Sandia fog facility[C]//Degraded Environments: Sensing, Processing, and Display 2017. *Int. Soc. Opt. Photonics* **2017**, *10197*, 1019704.
6. LaCasse, C.F.; Fuerschbach, K.H.; Craven, J.M. *Long Wave Infrared Spectropolarimetric Directional Reflectometer*; Sandia National Lab. (SNL-NM): Albuquerque, NM, USA; Sandia National Lab. (SNL-CA): Livermore, CA, USA, 2018.
7. Zeng, X.; Chu, J.; Cao, W. Visible–IR transmission enhancement through fog using circularly polarized light. *Appl. Opt.* **2018**, *57*, 6817–6822. [CrossRef] [PubMed]
8. Yang, B.; Yan, C.X. Multispectral polarization characteristics of marine aerosols. *Spectrosc. Spectr. Anal.* **2016**, *36*, 2736–2741.
9. Sun, X.M.; Wang, H.H.; Shen, J.; Wan, L. Study on the polarized light scattering properties of aerosols in the ocean background. *Adv. Lasers Optoelectron.* **2016**, *53*, 16–23.
10. Chen, W.; Sun, X.B.; Qiao, Y.L.; Chen, Z.T.; Yin, Y.L. Target polarization detection under the background of sea surface glare. *Infrared Laser Eng.* **2017**, *46*, 69–74.
11. Zhang, C.; Zhang, J.; Wu, X. Numerical analysis of light reflection and transmission in poly-disperse sea fog. *Opt. Express* **2020**, *28*, 25410–25430. [CrossRef] [PubMed]
12. Panchenko, M.V.; Polkin, V.V.; Terpugova, S.A. Testing the algorithms for taking into account relative humidity of air in the model of optical characteristics of absorbing aerosol. In Proceedings of the 21st International Symposium Atmospheric and Ocean Optics: Atmospheric Physics, Tomsk, Russian, 22–26 June 2015; Volume 9680, pp. 577–580.
13. Mao, Q.; Nie, X. Polarization performance of a polydisperse aerosol atmosphere based on vector radiative transfer model. *Atmos. Environ.* **2022**, *277*, 119079. [CrossRef]
14. Nie, X.; Mao, Q. Study on shortwave radiative transfer characteristics in polydisperse aerosols in a clear sky. *Infrared Phys. Technol.* **2021**, *118*, 103903. [CrossRef]
15. Wang, B.H. *Sea Fog*; Beijing Ocean Press: Beijing, China, 1983; pp. 101–123.
16. Zhang, J.W.; Zhang, S.P.; Wu, X.J. Research on Sea Fog in the Yellow Sea Based on MODIS—Inversion of Sea Fog Feature. *J. Ocean. Univ. China* **2009**, *39*, 311–318.
17. Bentz, B.Z.; Redman, B.J.; van der Laan, J.D. Light transport with weak angular dependence in fog. *Opt. Express* **2021**, *29*, 13231–13245. [CrossRef]
18. Liou, K.N. *An Introduction to Atmospheric Radiation*; Elsevier: Amsterdam, The Netherlands, 2002.